A novel *de novo* FEM1C variant as a potential cause of neurodevelopmental disorder with absent speech, pyramidal signs, and limb ataxia

Abhishek Anil Dubey[1]*, Magdalena Krygier[2]*, Natalia A. Szulc[1]*, Karolina Rutkowska[3], Joanna Kosińska[3], Agnieszka Pollak[3], Małgorzata Rydzanicz[3], Tomasz Kmieć[4], Maria Mazurkiewicz-Bełdzińska[2], Wojciech Pokrzywa[1#], Rafał Płoski[3#]

[1] Laboratory of Protein Metabolism, International Institute of Molecular and Cell Biology in Warsaw, 4 Ks. Trojdena Str., 02-109 Warsaw, Poland

[2] Department of Developmental Neurology, Medical University of Gdansk, ul. Debinki 7, 80-952, Gdansk, Poland

[3] Department of Medical Genetics, Medical University of Warsaw, Pawinskiego 3c, 02-106 Warsaw, Poland

[4] Department of Neurology and Epileptology, The Children's Memorial Health Institute, aleja Dzieci Polskich 20, 04-730 Warsaw, Poland.

Correspondence should be addressed to Rafal Ploski, Department of Medical Genetics, Medical University of Warsaw, Pawińskiego 3c, 02-106 Warsaw, Poland

Tel.: 0048 22 572 06 95, fax: 0048 22 572 06 96, e-mail: rafal.ploski@wum.edu.pl

and Wojciech Pokrzywa, Laboratory of Protein Metabolism, International Institute of Molecular and Cell Biology in Warsaw, 4 Ks. Trojdena Str., 02-109 Warsaw, Poland

Tel: 0048 22 597 07 43; e-mail: wpokrzywa@iimcb.gov.pl

* These authors contributed equally

Abstract

Maintaining protein homeostasis (proteostasis) requires the degradation of damaged or unwanted proteins and plays a crucial role in cellular function. The principal proteolytic component of the proteostasis network is the ubiquitin-proteasome system (UPS) which orchestrates protein degradation through ubiquitination of appropriate targets. Ubiquitination is mediated by an enzymatic cascade involving, i.e., E3 ubiquitin ligases, many of which belong to the cullin-RING ligases (CRLs) family. Genetic defects of the UPS are known causes of neurodevelopmental disorders, with >60 entities described so far. Using exome sequencing (ES) to diagnose a pediatric patient with global developmental delay, pyramidal signs, and limb ataxia, we identified a *de novo* missense variant c.376G>C; p.(Asp126His) in the *FEM1C* gene, which encodes a CRL substrate receptor. The p.(Asp126His) variant, which alters a conserved amino acid (phyloP100way = 7.9), is located within a highly constrained coding region (CCR=98.6) and is predicted to be pathogenic by the majority (13/19) of *in silico* tools. To further assess its pathogenicity, we employed *Caenorhabditis elegans* nematode as a disease model. We found that the mutant vs. wild-type worms had impaired mobility as assessed by track length (p=0.0001), turn counts (p=0.0001), and omega bend counts (p=0.038). Furthermore, mutant worms had histologically normal muscle architecture but were sensitive to an acetylcholinesterase inhibitor - aldicarb which indicates that their locomotion defects result from synaptic defects rather than muscle dysfunction. We conclude that the disease in our patient may be the first reported case of a neurodevelopmental disorder caused by the *FEM1C* genetic defect.

Introduction

Neurodevelopmental disorders (NDDs) are a group of neurological and psychiatric conditions that arise from disruption of brain development. The defining clinical features are impairments of motor skills, cognition, communication, and/or behavior. NDDs encompass a wide range of disabilities, such as developmental delay (DD), intellectual disability (ID), cerebral palsy (CP), autism spectrum disorder (ASD), attention deficit hyperactivity disorder (ADHD), epilepsy, and others. The etiology of NDDs is heterogeneous and includes multifactorial, acquired, and monogenic causes, the latter often caused by damaging *de novo* mutations (Deciphering Developmental Disorders, 2017; Thapar et al., 2017). Interestingly, whereas the pathogenesis of brain dysfunction in NDDs is still poorly understood, at least 62 forms of NDDs are caused by mutations in genes encoding components of the ubiquitin-proteasome system (UPS), especially E3 ubiquitin ligases (Ebstein et al., 2021).

Maintaining proteostasis requires the degradation of damaged or unwanted proteins and plays a crucial role in cellular function, organismal growth, and, ultimately, viability (Douglas & Dillin, 2010; Morimoto & Cuervo, 2014). The UPS orchestrates protein degradation in a process known as ubiquitination, where a small protein ubiquitin is covalently attached to its target (Kerscher et al., 2006). Ubiquitination is mediated by an enzymatic cascade involving ubiquitin-activating (E1), ubiquitin-conjugating (E2), and ubiquitin ligase (E3) enzymes (Komander, 2009). The proteasome complex recognizes ubiquitinated proteins and, through proteolysis, degrades them into short peptides that can be further processed (Hochstrasser, 1996). The majority of E3s belong to the RING family, and within it, the largest subfamily is the cullin-RING ligases (CRLs) (Nguyen et al., 2017). CRL complexes are large molecular

machinery consisting of a cullin protein that acts as a scaffold, a RING box protein coordinating ubiquitination, a substrate receptor that recruits the target protein, and adaptor proteins that link the substrate receptor to the cullin (Nguyen et al., 2017).

Here we describe an 8-year-old boy with severe DD, lack of speech, pyramidal signs, and limb ataxia. Whole exome sequencing (WES) identified a *de novo* missense variant c.376G>C; p.(Asp126His) in the *FEM1C* gene, which has not been yet associated with human disease. FEM1C acts as a CRL substrate receptor (Dankert et al., 2017), selectively recruiting target proteins upon recognition of a specific sequence motif termed degron. Both N- and C-terminus of proteins may yield destabilizing motifs, termed N- and C-degrons (Varshavsky, 2019), respectively, that are targeted by different E3s. The putative FEM1C disease-causing mutation p.(Asp126His) occurs within its degron-binding pocket, leading to an inability to mediate protein substrates turnover. Pathogenicity of the p.(Asp126His) variant found in the patient is supported by studies of nematode *Caenorhabditis elegans* with a corresponding mutation in FEM-1 (a worm homolog of human FEM1C), where the mutant animals also developed neurological dysfunction. In conclusion, we provide the first description of a neurodevelopmental disorder associated with a novel *FEM1C* mutation which has functional consequences for the nervous system in the *C. elegans* model.

Results

Exome sequencing and family studies

WES performed in the proband revealed three ultra-rare (0 frequency in gnomAD v3.1.2 https://gnomad.broadinstitute.org and an in-house database of >5500 Polish exomes) heterozygous missense variants in *CSMD2*, *RALYL* and *FEM1C* genes which were selected for family study. Variants in both *CSMD2* and *RALYL* were found to be inherited from a healthy mother and father and thus were considered as not disease-causing. The *FEM1C* variant (hg38, chr5:115543118-C>G, NM_020177.3:c.376G>C, p.(Asp126His), Fig. 1A) was absent in both parents, indicating a *de novo* event (Fig. 1B). The *FEM1C* p.(Asp126His) was predicted as damaging by 13 different pathogenicity predictors implemented in the Varsome web server (https://varsome.com), including BayesDel addAF, BayesDel noAF, EIGEN, EIGEN PC, FATHMM-MKL, FATHMM-XF, LRT, M-CAP, MutPred, MutationTaster, PROVEAN, PrimateAI, SIFT, and as “Tolerated” by six other predictors (DEOGEN2, FATHMM, LIST-S2, MVP, Mutation assessor, SIFT4G). The c.376G position is highly conserved (PhastCons100way score 1.0, GERP++ value 5.5), and the p.(Asp126His) variant affects the conserved Asp126 residue located in the ankyrin repeat domain ANK4 (phyloP100way = 7.9). Moreover, *FEM1C* p.(Asp126His) variant is located in a highly constrained coding region (CCR=98,6). The scarcity of coding variants in the proximity of p.(Asp126His), characteristic of CCR, is illustrated in Fig. 1C**,** based on the gnomAD and Bravo datasets.

The nematode *C. elegans* as a model to study the functional consequences of the FEM1C p.(Asp126His) mutation

The degron-binding pocket of FEM1C is located within its N-terminal ankyrin domain (Chen et al., 2021; Yan et al., 2021) (Fig. 2A), a well-conserved motif in all FEM1 proteins and their orthologs in other organisms, including *C. elegans* nematode. *C. elegans* is a well-established model organism to study multiple human diseases, including neurodegeneration and ataxias (Alexander et al., 2014; Sorkaç et al., 2016). Therefore, we used worms to investigate the

physiological impact of the FEM1C p.(Asp126His) mutation. The sequence alignment of degron-binding regions of FEM1C and its *C. elegans* ortholog FEM-1 showed high evolutionary conservation, including the critical Asp126 position (Asp133 in worms) (Fig. 2B). We also compared structures of both proteins, as protein folding directly underlies molecular interactions and may point to the conserved functional role. Superposition of the experimental structure of the FEM1C degron-binding region (residues 1-390) and model of its FEM-1 analog obtained from the AlphaFold database (Jumper et al., 2021; Varadi et al., 2021) showed very high structural similarity, evidenced in particular by a low value (1.213 Å) of root-mean-square deviation.

Recent structural studies of the FEM1C basis of degron recognition pointed to the critical role of several residues (Chen et al., 2021; Yan et al., 2021). Therefore, we compared their evolutionary conservation to assess the similarity of the degron-binding pocket between humans and *C. elegans*. Among 15 residues of FEM1C indicated as involved in Arg/C degron binding of its substrate SIL1 (Chen et al., 2021), 13 were conserved both in sequence and structure in FEM-1 (Fig. 2B, 2C). Notably, the two differing residues showed similar physicochemical properties (phenylalanine/tyrosine and lysine/arginine), further supporting the high conservation of the degron binding pocket and indicating a likely similar substrate pool of FEM1C and FEM-1.

Thus, the high similarity of the degron-binding pocket between human FEM1C and its worm ortholog, as well as conservation of Asp126 residue, are strong premises to employ *C. elegans* as a FEM1C p.(Asp126His) disease model.

C. elegans FEM-1^{Asp133His} mutants develop locomotor defects due to neuronal dysfunction

Ataxias are a heterogeneous group of disorders in which cerebellar dysfunction underlies neurological symptoms such as impaired muscle coordination (Shakkottai & Paulson, 2009). As pyramidal signs and limb ataxia were prominent symptoms in our proband, we examined the locomotion behavior of worms expressing the putative disease-causing FEM-1^{Asp133His} mutant protein (hereafter *fem-1* mutants) generated using the CRISPR/Cas9 gene-editing tool (Fig. 2D). Locomotion is a complex reflection of the functionality of the *C. elegans* nervous system. It encompasses a range of motor activities, such as omega bends (deep bends usually on the ventral side of the body that change the movement direction) and reversals (transition from crawling forward to crawling backwards). Using WormLab System (MBF Bioscience), we measured animal locomotor parameters in wild-type and *fem-1* worms in detail. We found that the *fem-1* mutants had impaired mobility as assessed by track length and turn counts (p=0.0001, Fig. 2E). In particular, the *fem-1* mutants experienced difficulty performing omega bends (p=0.038) but showed no defects in reversals (P=0.734, Fig. 2E). This suggests a functional deficit of distinct neurons in *fem-1* mutants, as the execution of reversals and omega bends is encoded by separate neurons (Gray et al., 2005).

The organization of sarcomeres and their components in *C. elegans* body wall muscles is a highly evolutionary conserved feature (Gieseler et al., 2017). To determine whether locomotion defects in *fem-1* mutants occur due to the loss of muscle fiber structure, we performed phalloidin staining of F-actin filaments containing I bands (Shai, S., Methods in cell biology (January 12, 2006), WormBook, ed. The *C. elegans* Research Community,

WormBook, 10.1895/wormbook.1.49.1, http://www.wormbook.org). We did not find myofilament disorganization or reduced muscle cell size in *fem-1* mutants (Fig. 2F), suggesting that the observed deficits in locomotion are not the result of compromised body wall muscle organization.

The aldicarb (an acetylcholinesterase inhibitor) induced paralysis assay identifies abnormal synaptic transmission in the *C. elegans* mutant of interest (Oh & Kim, 2017; Sorkaç et al., 2016). We performed an aldicarb sensitivity assay to confirm that the mobility phenotype observed in the *fem-1* mutants is due to neuronal dysfunction. We found that the *fem-1* mutants were significantly more sensitive to aldicarb than wild-type worms (p=0.0023, Fig. 2G), indicating that their locomotion impairment is due to synaptic defects rather than muscle dysfunction.

Discussion

We describe a pediatric case of severe DD, lack of speech, pyramidal signs and limb ataxia associated with a novel *de novo* variant p.(Asp126His) in the *FEM1C* gene. The variant altered a conserved amino acid position and was predicted to be pathogenic by most *in silico* tools. Moreover, the variant is located within a highly constrained coding region, i.e., a region with a scarcity of coding variation observed among healthy people. Such regions are enriched in pathogenic variants for autosomal dominant disorders (Havrilla et al., 2019).

Pathogenicity of the p.(Asp126His) variant found in our patient is further supported by studies of transgenic *C. elegans,* a well-established model organism to study multiple human diseases, including neurodegeneration and ataxias (Alexander et al., 2014; Sorkaç et al., 2016). We found that the patient's allele reduced animal mobility by affecting omega bends but not reversals. This effect suggests a functional deficit of distinct neurons in *fem-1* mutants, as the execution of reversals and omega bends is encoded by separate neurons (Gray et al., 2005). We also found that mutant worms had normal muscle architecture and were sensitive to an acetylcholinesterase inhibitor - aldicarb which further supports that that locomotion defects caused by a mutation in the *fem-1* gene result from neuronal synaptic defects.

Recent studies demonstrated that human FEM1 proteins (FEM1A, FEM1B, and FEM1C) recognize distinct motifs ending with arginine (Arg/C-degrons) (Koren et al., 2018; Lin et al., 2018). The putative FEM1C disease-causing mutation p.(Asp126His) occurs within its degron-binding pocket and impacts a residue directly involved in binding the critical C-terminus arginine of FEM1C substrates. Moreover, FEM1C^{Asp126Ala} mutation was shown previously to abolish or severely abrogate substrate binding emphasizing its essential role in Arg/C-degron recognition (Chen et al., 2021; Yan et al., 2021). We hypothesize that impaired degron recognition resulting from FEM1C^{Asp126His} mutation and its consequent inability to mediate ubiquitination of specific substrates might be the molecular mechanism of the patient's disease. Therefore, it would be crucial to perform proteomic studies on the patient's material to look for proteins with elevated levels and containing relevant degron motifs as likely substrates of FEM1C, whose dysregulation may be responsible for the disease.

Importantly, our results indicate the functional effect of p.(Asp126His) on FEM1C function in *C. elegans.* The *fem-1* gene was originally identified in *C. elegans*. FEM-1 through

ubiquitination and degradation of sex-determining proteins is vital in worm gender regulation (Doniach & Hodgkin, 1984; Starostina et al., 2007). Interestingly, our *fem-1* mutant worms did not show sex determination defects (data not shown), suggesting that the defect conferred by mutation shows considerable tissue-specificity.

In conclusion, we have identified neurodevelopmental disorders associated with a novel *FEM1C* mutation that exerts functional consequences on the nervous system in a *C. elegans* model.

Materials and Methods

Clinical report

The patient is the first child of non-consanguineous parents. The family history was unremarkable. The pregnancy was uncomplicated, with normal screening ultrasounds. He was delivered at term via C-section, and all mensuration at birth was normal. Developmental concerns became apparent to the family at around six months of age due to gross motor delay. Neurologic evaluation at nine months of age was notable for axial hypotonia and increased muscle tone in the lower limbs with brisk tendon reflexes. Magnetic Resonance Imaging (MRI) of the brain with spectroscopy performed at the age of 11 months showed symmetrical enlargement of the posterior horns of the lateral ventricles. The boy could not sit independently until 2,5 years of age and crawl until three years. Brain MRI at the age of four showed mildly enlarged lateral ventricles comparable to the previous examination and small areas of incomplete myelination at the posterior parts of the lateral ventricles. A recent neurological examination at the age of eight was notable for global developmental delay, lack of speech, ataxia, and pyramidal signs. Anthropometric measurements were normal, including height, weight, and head circumference. The patient had a cheerful attitude, reacted to simple commands, and communicated using assistive devices. He was not able to walk independently. He stood with support and crossed his legs when held by the caregiver. There was massive nystagmus in all directions of gaze, left divergent strabismus, cerebellar signs in the upper limbs (ataxia, intention tremor, dysmetria, dysdiadochokinesia), axial hypotonia, pyramidal signs (spasticity with brisk deep tendon reflexes in the upper and lower limbs), and bilateral *pes planovalgus.* Results of metabolic evaluation, including urine organic acid analysis, tandem mass spectrometry screening, and neurotransmitters in cerebrospinal fluid, were normal. Chromosomal microarray did not show any disease-causing copy number variants.

Genetic study

Whole exome sequencing (WES) was conducted for the proband only using DNA purified from the whole blood. According to the manufacturer's instructions, the library was constructed using SureSelect All Human Exon V7 (Agilent Technologies, Cedar Creek, TX, USA). The library was paired-end sequenced (2x100 bo) on HiSeq 1500 (Illumina, San Diego, CA, USA) to the mean depth > 100x (the min. 10x coverage was 96.7%, and 20x - 91.6%). Reads were aligned to the GRCh38 (hg38) reference genome. Data analysis and variants prioritization was performed as previously described (Rydzanicz et al., 2021). Variants considered causative were validated in the proband and studied in his parents by amplicon deep sequencing (ADS)

performed using Nextera XT Kit (Illumina) and paired-end sequencing as described above for WES.

Worm maintenance and strains

Worms were maintained on nematode growth medium (NGM) plates seeded with OP50 *Escherichia coli* bacteria at 20°C unless otherwise stated (Brenner, 1974). Wild-type nematodes were the N2 (Bristol) strain. PHX5163 *fem-1(syb5163)* mutant worms were generated at SunyBiotech (http://www.sunybiotech.com) by CRISPR/Cas9 methodology using the sgRNAs sg1-CCA TTA AGA GGT GCA TGT TAC GA and sg2-TTA AGA GGT GCA TGT TAC GAT G. The editing was confirmed by sequencing (Fig. 2D). Strain PHX5163 was outcrossed 2X to N2 to generate strain WOP497.

Worm mobility assay

Day 1 adult worms were placed onto a single NGM plate, and worm movements were recorded for 2 minutes using the WormLab system (MBF Bioscience), keeping the frame rate, exposure time, and gain set to 7.5 frames per second. Parameters such as the track length, turn count, number of reversals, and reversal distance travelled pattern of individual worms were recorded and analyzed using the WormLab software (MBF Bioscience). 75 worms from were recorded for one biological replicate. The assay consisted of three independent biological replicates.

Phalloidin staining

Sarcomere assembly was monitored by staining F-actin with Phalloidin-Atto 390 (Sigma Aldrich) using the protocol described in Romani and Auwerx (2021). Briefly, synchronized Day 1 adults were washed, and the worm pellet was snap frozen in liquid nitrogen. The pellet was dried in the SpeecVac concentrator followed by worm permeabilization using 100% ice-cold acetone for 5 minutes. After acetone removal, the worm pellet was stained using Phalloidin-Atto 390 for 30 minutes in the dark. Stained worms were washed twice and mounted onto a 2% (w/v) agarose pad on a glass slide and imaged on Zeiss LSM800 inverted confocal microscope.

Aldicarb sensitivity assay

Aldicarb sensitivity assay was performed as described in Sorkaç et al. (2016). Briefly, 20 adult day 1 worms were placed on 1 mM aldicarb, and worm paralysis was assessed by their inability to move within 5 seconds in response to touch in the head and tail region. Paralysis was assessed every 20 minutes until all worms were completely paralyzed. The assay consisted of three independent biological replicates.

Acknowledgements

We thank the *Caenorhabditis* Genetics Centre (funded by the NIH National Centre for Research Resources, P40 OD010440) for the N2 strain and OP50 *E. coli*.

Funding

A.A.D. and W.P. were funded by the Norwegian Financial Mechanism 2014-2021 and operated by the Polish National Science Centre, Poland, under the project contract number UMO-2019/34/H/NZ3/00691. N.A.S. was founded by the National Science Centre, Poland, grant PRELUDIUM number 2021/41/N/NZ1/03473.

Conflict of Interest Statement

The authors have declared no competing interest.

References

Alexander, A. G., Marfil, V., & Li, C. (2014). Use of Caenorhabditis elegans as a model to study Alzheimer's disease and other neurodegenerative diseases [Review]. *Frontiers in Genetics*, *5*. https://doi.org/10.3389/fgene.2014.00279

Brenner, S. (1974). The genetics of Caenorhabditis elegans. *Genetics*, *77*(1), 71-94. https://doi.org/10.1093/genetics/77.1.71

Chen, X., Liao, S., Makaros, Y., Guo, Q., Zhu, Z., Krizelman, R., Dahan, K., Tu, X., Yao, X., Koren, I., & Xu, C. (2021). Molecular basis for arginine C-terminal degron recognition by Cul2FEM1 E3 ligase. *Nature Chemical Biology*, *17*(3), 254-262. https://doi.org/10.1038/s41589-020-00704-3

Dankert, J. F., Pagan, J. K., Starostina, N. G., Kipreos, E. T., & Pagano, M. (2017). FEM1 proteins are ancient regulators of SLBP degradation. *Cell Cycle*, *16*(6), 556-564. https://doi.org/10.1080/15384101.2017.1284715

Deciphering Developmental Disorders, S. (2017). Prevalence and architecture of de novo mutations in developmental disorders. *Nature*, *542*(7642), 433-438. https://doi.org/10.1038/nature21062

Doniach, T., & Hodgkin, J. (1984). A sex-determining gene, fem-1, required for both male and hermaphrodite development in Caenorhabditis elegans. *Dev Biol*, *106*(1), 223-235. https://doi.org/10.1016/0012-1606(84)90077-0

Douglas, P. M., & Dillin, A. (2010). Protein homeostasis and aging in neurodegeneration. *J Cell Biol*, *190*(5), 719-729. https://doi.org/10.1083/jcb.201005144

Ebstein, F., Kury, S., Papendorf, J. J., & Kruger, E. (2021). Neurodevelopmental Disorders (NDD) Caused by Genomic Alterations of the Ubiquitin-Proteasome System (UPS): the Possible Contribution of Immune Dysregulation to Disease Pathogenesis. *Front Mol Neurosci*, *14*, 733012. https://doi.org/10.3389/fnmol.2021.733012

Gieseler, K., Qadota, H., & Benian, G. M. (2017). Development, structure, and maintenance of C. elegans body wall muscle. *WormBook*, *2017*, 1-59. https://doi.org/10.1895/wormbook.1.81.2

Gray, J. M., Hill, J. J., & Bargmann, C. I. (2005). A circuit for navigation in Caenorhabditis elegans. *Proc Natl Acad Sci U S A*, *102*(9), 3184-3191. https://doi.org/10.1073/pnas.0409009101

Havrilla, J. M., Pedersen, B. S., Layer, R. M., & Quinlan, A. R. (2019). A map of constrained coding regions in the human genome. *Nat Genet*, *51*(1), 88-95. https://doi.org/10.1038/s41588-018-0294-6

Hochstrasser, M. (1996). UBIQUITIN-DEPENDENT PROTEIN DEGRADATION. *Annual Review of Genetics*, *30*(1), 405-439. https://doi.org/10.1146/annurev.genet.30.1.405

Jumper, J., Evans, R., Pritzel, A., Green, T., Figurnov, M., Ronneberger, O., Tunyasuvunakool, K., Bates, R., Žídek, A., Potapenko, A., Bridgland, A., Meyer, C., Kohl, S. A. A., Ballard, A. J., Cowie, A., Romera-Paredes, B., Nikolov, S., Jain, R., Adler, J., . . . Hassabis, D. (2021). Highly accurate protein structure prediction with AlphaFold. *Nature*, *596*(7873), 583-589. https://doi.org/10.1038/s41586-021-03819-2

Kerscher, O., Felberbaum, R., & Hochstrasser, M. (2006). Modification of proteins by ubiquitin and ubiquitin-like proteins. *Annu Rev Cell Dev Biol*, *22*, 159-180. https://doi.org/10.1146/annurev.cellbio.22.010605.093503

Komander, D. (2009). The emerging complexity of protein ubiquitination. *Biochem Soc Trans*, *37*(Pt 5), 937-953. https://doi.org/10.1042/BST0370937

Koren, I., Timms, R. T., Kula, T., Xu, Q., Li, M. Z., & Elledge, S. J. (2018). The Eukaryotic Proteome Is Shaped by E3 Ubiquitin Ligases Targeting C-Terminal Degrons. *Cell*, *173*(7), 1622-1635.e1614. https://doi.org/10.1016/j.cell.2018.04.028

Lin, H. C., Yeh, C. W., Chen, Y. F., Lee, T. T., Hsieh, P. Y., Rusnac, D. V., Lin, S. Y., Elledge, S. J., Zheng, N., & Yen, H. S. (2018). C-Terminal End-Directed Protein Elimination by CRL2 Ubiquitin Ligases. *Mol Cell*, *70*(4), 602-613 e603. https://doi.org/10.1016/j.molcel.2018.04.006

Liu, W., Xie, Y., Ma, J., Luo, X., Nie, P., Zuo, Z., Lahrmann, U., Zhao, Q., Zheng, Y., Zhao, Y., Xue, Y., & Ren, J. (2015). IBS: an illustrator for the presentation and visualization of biological sequences. *Bioinformatics*, *31*(20), 3359-3361. https://doi.org/10.1093/bioinformatics/btv362

Madeira, F., Pearce, M., Tivey, A. R. N., Basutkar, P., Lee, J., Edbali, O., Madhusoodanan, N., Kolesnikov, A., & Lopez, R. (2022). Search and sequence analysis tools services from EMBL-EBI in 2022. *Nucleic Acids Res*. https://doi.org/10.1093/nar/gkac240

Morimoto, R. I., & Cuervo, A. M. (2014). Proteostasis and the aging proteome in health and disease. *J Gerontol A Biol Sci Med Sci*, *69 Suppl 1*, S33-38. https://doi.org/10.1093/gerona/glu049

Nguyen, H. C., Wang, W., & Xiong, Y. (2017). Cullin-RING E3 Ubiquitin Ligases: Bridges to Destruction. *Subcell Biochem*, *83*, 323-347. https://doi.org/10.1007/978-3-319-46503-6_12

Oh, K. H., & Kim, H. (2017). Aldicarb-induced Paralysis Assay to Determine Defects in Synaptic Transmission in Caenorhabditis elegans. *Bio Protoc*, *7*(14). https://doi.org/10.21769/BioProtoc.2400

Romani, M., & Auwerx, J. (2021). Phalloidin Staining of Actin Filaments for Visualization of Muscle Fibers in Caenorhabditis elegans. *Bio Protoc*, *11*(19), e4183. https://doi.org/10.21769/BioProtoc.4183

Rydzanicz, M., Zwolinski, P., Gasperowicz, P., Pollak, A., Kostrzewa, G., Walczak, A., Konarzewska, M., & Ploski, R. (2021). A recurrent de novo variant supports KCNC2 involvement in the pathogenesis of developmental and epileptic encephalopathy. *Am J Med Genet A*, *185*(11), 3384-3389. https://doi.org/10.1002/ajmg.a.62455

Shai, S., Methods in cell biology (January 12, 2006), *WormBook,* ed. T. *C. e.* R. Community, WormBook, 10.1895/wormbook.1.49.1, http://www.wormbook.org

Shakkottai, V. G., & Paulson, H. L. (2009). Physiologic alterations in ataxia: channeling changes into novel therapies. *Arch Neurol*, *66*(10), 1196-1201. https://doi.org/10.1001/archneurol.2009.212

Sorkaç, A., Alcantara, I. C., & Hart, A. C. (2016). In Vivo Modelling of ATP1A3 G316S-Induced Ataxia in C. elegans Using CRISPR/Cas9-Mediated Homologous Recombination Reveals Dominant Loss of Function Defects. *PLOS ONE*, *11*(12), e0167963. https://doi.org/10.1371/journal.pone.0167963

Starostina, N. G., Lim, J.-m., Schvarzstein, M., Wells, L., Spence, A. M., & Kipreos, Edward T. (2007). A CUL-2 Ubiquitin Ligase Containing Three FEM Proteins Degrades TRA-1 to Regulate C. elegans Sex Determination. *Developmental Cell*, *13*(1), 127-139. https://doi.org/https://doi.org/10.1016/j.devcel.2007.05.008

Thapar, A., Cooper, M., & Rutter, M. (2017). Neurodevelopmental disorders. *Lancet Psychiatry*, *4*(4), 339-346. https://doi.org/10.1016/S2215-0366(16)30376-5

Varadi, M., Anyango, S., Deshpande, M., Nair, S., Natassia, C., Yordanova, G., Yuan, D., Stroe, O., Wood, G., Laydon, A., Žídek, A., Green, T., Tunyasuvunakool, K., Petersen, S., Jumper, J., Clancy, E., Green, R., Vora, A., Lutfi, M., . . . Velankar, S. (2021). AlphaFold Protein Structure Database: massively expanding the structural coverage of protein-sequence space with high-accuracy models. *Nucleic Acids Research*, *50*(D1), D439-D444. https://doi.org/10.1093/nar/gkab1061

Varshavsky, A. (2019). N-degron and C-degron pathways of protein degradation. *Proc Natl Acad Sci U S A*, *116*(2), 358-366. https://doi.org/10.1073/pnas.1816596116

Waterhouse, A. M., Procter, J. B., Martin, D. M. A., Clamp, M., & Barton, G. J. (2009). Jalview Version 2—a multiple sequence alignment editor and analysis workbench. *Bioinformatics*, *25*(9), 1189-1191. https://doi.org/10.1093/bioinformatics/btp033

Yan, X., Wang, X., Li, Y., Zhou, M., Li, Y., Song, L., Mi, W., Min, J., & Dong, C. (2021). Molecular basis for ubiquitin ligase CRL2FEM1C-mediated recognition of C-degron. *Nature Chemical Biology*, *17*(3), 263-271. https://doi.org/10.1038/s41589-020-00703-4

Legends to Figures

Figure 1. Results of genetic study.
A. Missense p.(Asp126His) variant in *FEM1C* gene identified in the proband by WES (coverage 119x, reads with alternate allele 57). **B.** Amplicon deep sequencing-based family study of p.(Asp126His) (P - proband: coverage 6459x, reads with alternate allele 3097, M - mother: coverage 6171x, reads with alternate allele 0, F – father: coverage 5931, reads with alternate allele 0). **C**. Overview of genetic variation in the proximity of p.(Asp126His) in a healthy population (GnomAD and Bravo cohorts, based on https://varsome.com).

Figure 2. Computational and functional analysis of the *C. elegans fem-1* mutant. **A.** Scheme of the domain architecture of human FEM1C visualized using the IBS software (Liu et al., 2015). ANK - ankyrin repeat; TPR - tetratricopeptide repeat; VHL box - von Hippel–Lindau box. Modified from Chen et al. (2021). **B.** Global alignment of binding regions of human FEM1C (residues 70-220; UniProt ID: Q96JP0) and *C. elegans* FEM-1 (residues 76-227; UniProt ID: P17221). Sequences were aligned using the EMBOSS Needle web server (Madeira et al., 2022) with default parameters and visualized in the Jalview Desktop software (Waterhouse et al., 2009) with residues colored by their physicochemical properties; D126/D133 position was indicated by arrow **C.** Comparison of residues involved in SIL1 Arg/C degron binding in FEM1C (cyan; PDB code: 6LBN) and FEM-1 (magenta; AlphaFold model corresponding to P17221). FEM-1 residues that differ from FEM1C were marked in yellow; the D126/D133 position was indicated by the arrow. **D.** Sequencing chromatogram of CRISPR/Cas9-generated FEM-1^{Asp133His} mutation displaying sequence peaks and base calls. Data visualized in the SnapGene 6 software (from Insightful Science; available at snapgene.com). **E.** The graphs show the track lengths, turn counts, number of reversals and omega bends (wild-type n=146 and FEM-1^{Asp133His} n=148*; N*=3*)*. *n* represents the number of worms; *N* represents the number of experimental repeats. The stars denote the levels of significance as per the *p-value* obtained by the Mann–Whitney test*. p-values* are shown adjacent to the respective graphs (ns - not significant, *$p \leq 0.05$, ***$p \leq 0.001$, ****$p \leq 0.0001$), dashes represent median of collective data from three independent biological replicates. Data plotted and analyzed in the GraphPad Prism 9 software. **F.** Phalloidin staining of F-actin-containing I-bands of wild-type (N2) and FEM-1^{Asp133His} expressing worms. Dashed lines separate two body wall muscle cells. The scale bar is 50 µm. **G.** Aldicarb sensitivity assay of wild-type (n=180) and FEM-1^{Asp133His} (n=171) worms; N=3. *n* represents the number of worms; *N* represents the number of experimental repeats. *p-value* was calculated using the Log-rank (Mantel-Cox) test. Data plotted and analyzed in the GraphPad Prism 9 software.

Abbreviations

ADHD - attention deficit hyperactivity disorder
ADS - amplicon deep sequencing
ASD - autism spectrum disorder
CCR - constrained coding region
CP - cerebral palsy
CRLs - cullin-RING ligases
DD - developmental delay
E1 - ubiquitin-activating enzyme
E2 - ubiquitin-conjugating enzyme
E3 - ubiquitin ligase
ES - exome sequencing
ID - intellectual disability
NDDs - neurodevelopmental disorders
NGM - nematode growth medium
UPS - ubiquitin-proteasome system
WES - whole exome sequencing

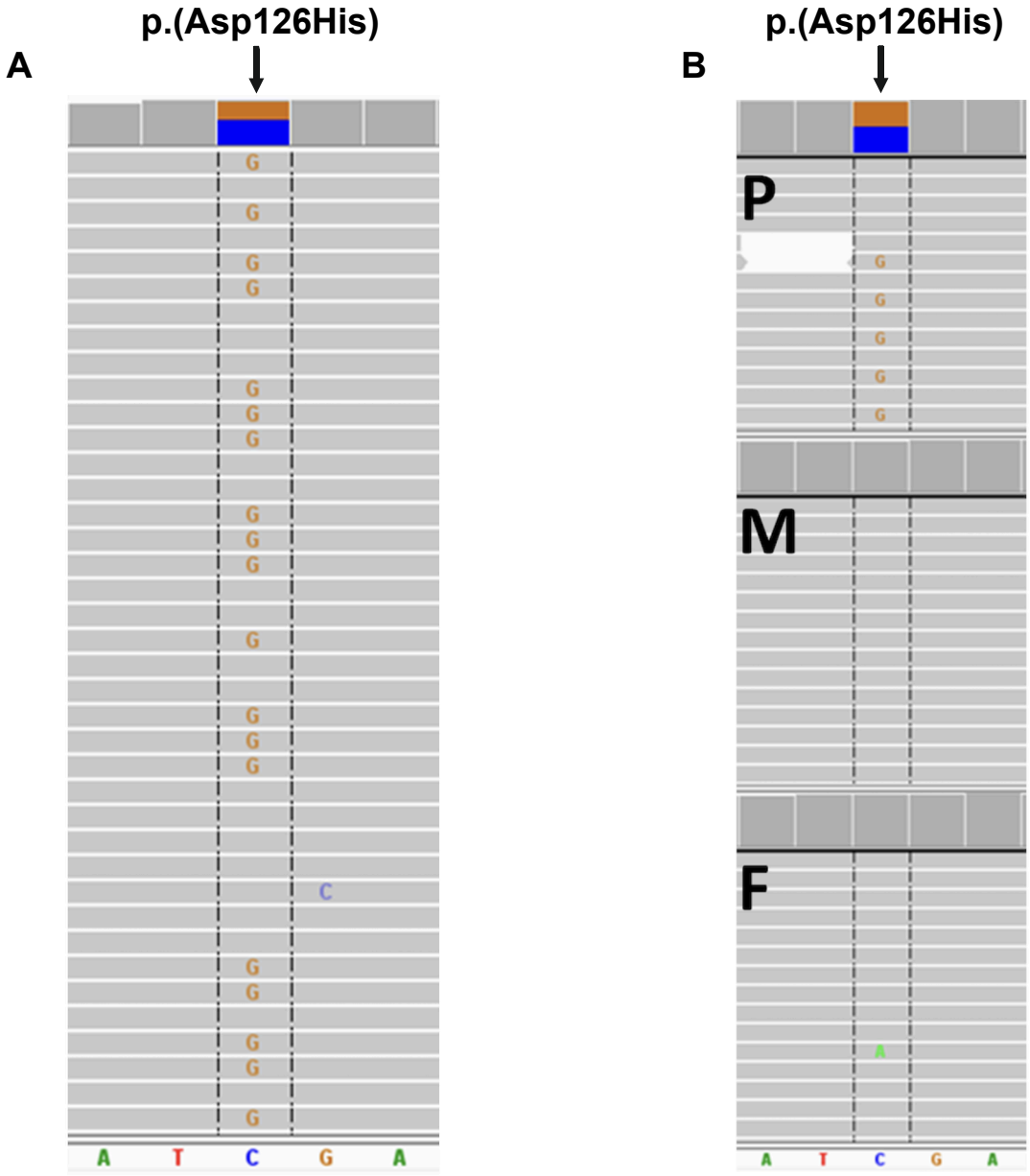

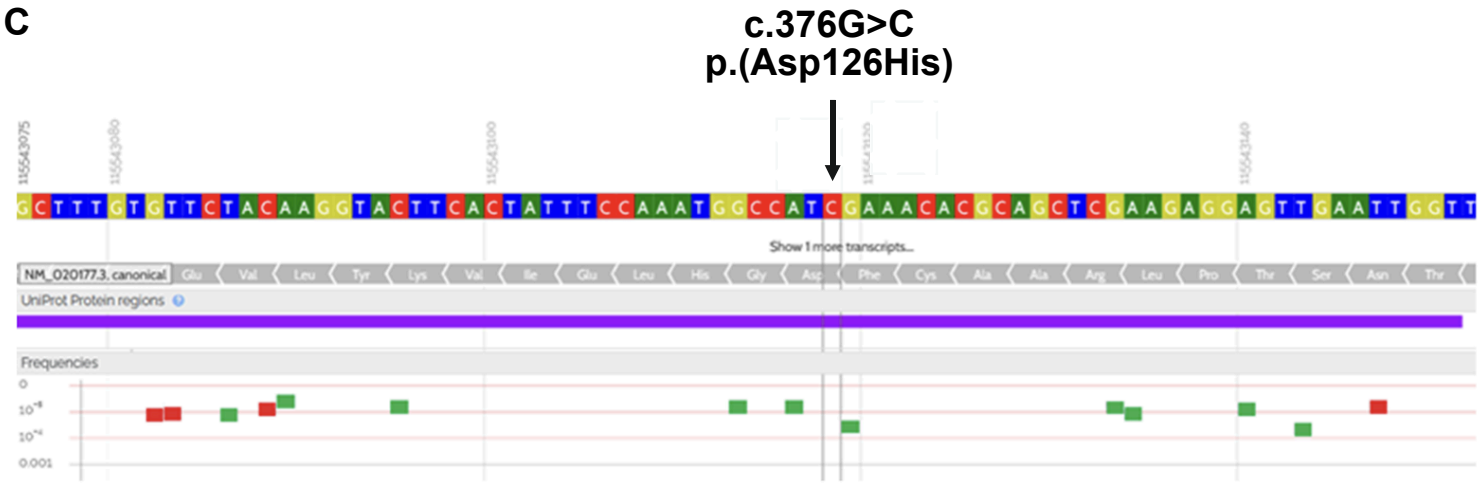

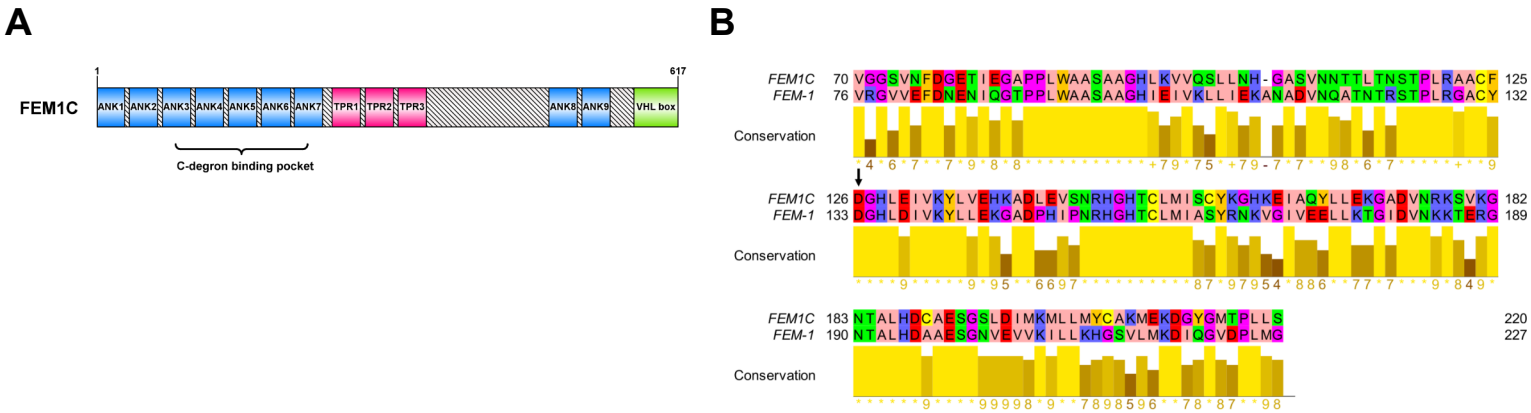

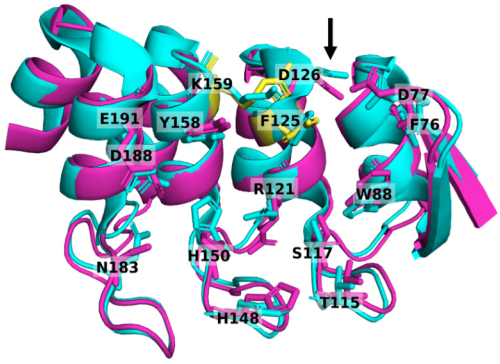

similarities	human	F76 D77 W88 T115 S117 R121 **D126** H148 H150 Y158 N183 D188 E191
	worm	F82 D83 W94 T122 S124 R128 **D133** H155 H157 Y165 N190 D195 E198
differences	human	F125 K159
	worm	Y132 R166